Solar Energy Materials & Solar Cells 273 (2024) 112953

Contents lists available at ScienceDirect

Solar Energy Materials and Solar Cells

journal homepage: www.elsevier.com/locate/solmat

The impact of interface recombination on the external quantum efficiency of silicon solar cells

Qing Yang [a,b], Karsten Bittkau [a], Alexander Eberst [a,b], Uwe Rau [a,b,*], Kaining Ding [a,b,**]

[a] IEK-5 Photovoltaics, Forschungszentrum Jülich GmbH, Wilhelm-Johnen Straße, 52425, Jülich, Germany
[b] Jülich Aachen Research Alliance (JARA-Energy) and Faculty of Electrical Engineering and Information Technology, RWTH Aachen University, Schinkelstr. 2, 52062, Aachen, Germany

ARTICLE INFO

Keywords:
Interface passivation
Surface recombination velocity
External quantum efficiency
Optical response enhancement
Silicon solar cell

ABSTRACT

In various types of organic/inorganic solar cells, optical response enhancement is consistently observed within the external quantum efficiency spectra owing to the improvement in interface passivation and the suppression of carrier recombination. In this study, we focused on crystalline silicon solar cells and systematically investigated the impact of interface recombination on the optical response upon dual-side illumination using numerical simulations. The results shed light on the interesting phenomenon that the surface recombination velocity has a significant impact on the external quantum efficiency, and it changes as the illumination direction changes. Moreover, from a practical perspective, the spectra of external quantum efficiency under dual-side illumination conditions can act as a powerful tool for the quick diagnosis of the passivation quality at the top and bottom interfaces.

1. Introduction

Organic/inorganic solar cells [1] with high efficiency and low cost have received significant attention in recent years and are widely demanded in our lives. To obtain extraordinary photovoltaic conversion efficiency, it is, among others, necessary to maximize the number of electrons collected per photon incident on the solar cells, which is characterized by the spectrally resolved external quantum efficiency (EQE) defined as the ratio between the number of charge carriers collected by the solar cell and the number of photons falling vertically on a solar cell area for each wavelength. Hence, EQE provides a comprehensive assessment of the solar cell's ability to convert incident light into electricity [2]. As a common means of optical characterization, EQE measurements are nondestructive and can be performed on fully assembled photovoltaic devices. In the ideal Shockley-Queisser case [2], when the photon energy is greater than or equal to the bandgap of the light absorber, EQE is equal to 1. However, under the practical operating conditions of solar cells, three factors result in EQE <1: (i) reflection losses, (ii) parasitic absorption, and (iii) recombination losses [2]. The combined effects of reflection and absorption can be collectively referred to as the optical loss.

Flat EQE spectra at high level is essentially demanded in highly efficient solar cells. Owing to the strong interplay between the optical and electrical properties inherent to key materials, it is more practical to reduce recombination losses by improving the passivation quality rather than by directly adjusting the optical characteristics. Salome et al. [3] passivated the rear interface within thin-film solar cells using an aluminum oxide (Al_2O_3) nanopatterned layer between Mo and Cu(In, Ga)Se_2 (CIGS). From the comparison of EQE spectra upon top illumination, the passivated device exhibits a superior optical response in the long-wavelength range above 500 nm compared to the reference cell. McVay et al. [4] reported a similar passivation strategy using Al_2O_3 coatings on the top surface of Pt/Tungsten diselenide (WSe_2) vertical Schottky junction solar cells. It was observed that the optical response was enhanced across the entire wavelength range within the EQEs under top illumination, suggesting that this wavelength-dependent enlargement is attributed to surface doping as well as the reduction in surface recombination due to the passivation of traps. Hatamvand et al. [5] studied the single-side and dual-side interfacial passivation of the perovskite light absorbing layer on perovskite solar cells with a standard structure (n-i-p) by applying Naphthylmethylammonium Iodide (NMAI) salt as passivation layer at the rear interface of perovskite/electron

* Corresponding author. IEK-5 Photovoltaics, Forschungszentrum Jülich GmbH, Wilhelm-Johnen Straße, 52425, Jülich, Germany.
** Corresponding author. IEK-5 Photovoltaics, Forschungszentrum Jülich GmbH, Wilhelm-Johnen Straße, 52425, Jülich, Germany.
E-mail addresses: u.rau@fz-juelich.de (U. Rau), k.ding@fz-juelich.de (K. Ding).

https://doi.org/10.1016/j.solmat.2024.112953
Received 22 April 2024; Received in revised form 17 May 2024; Accepted 18 May 2024
Available online 23 May 2024

transporting layer (ETL) and the front interface of perovskite/hole transporting layer (HTL). The NMAI-passivated devices (rear-, front- and dual-side) exhibited a significantly higher EQE response over the entire wavelength range compared to their control counterparts upon bottom illumination. Ding et al. [6] improved rear interface passivation for silicon heterojunction (SHJ) solar cells by increasing the thickness of intrinsic hydrogenated amorphous silicon oxide layer (a-SiO_X:H <i>). Upon top illumination, an increase in the EQE at long wavelengths was observed because of the improvement in the passivation quality of the c-Si/a-SiO_X:H rear interface, implying that a thicker buffer layer reduced recombination losses at the rear interface.

From numerous studies related to organic/inorganic solar cells, we observed that the improvement in interface passivation was often accompanied by an enhancement of the optical response. For some cases of interface passivation, the optical response enhancement only occurred in the long-wavelength range, whereas in other cases, the optical response across the entire spectrum was elevated. These results are universally present and are independent of the solar cell type. However, little effort has been devoted to shed light on this issue. In the present study, we elaborate on the mechanism behind the spectrally dependent surface recombination. Herein, we gain an original insight into this issue by relying on numerical simulations conducted with Quokka 3 [7–9], which numerically solved the 3D charge carrier transport in silicon devices in a quasi-neutral state with satisfactory precision [10–12]. We investigated the interplay between (i) the wavelength region of EQE response enhancement (long wavelength or entire range), (ii) the location of the passivated interface (front-sided or rear-sided), and (iii) the illumination direction during EQE measurements (top or bottom). Therefore, we modeled two silicon solar cells with a p-n junction on the front and rear surfaces, and calculated the EQE spectra with various surface recombination velocities at both the front and rear interfaces upon dual-side illumination.

2. Results and discussion

The cross-sections of the two silicon solar cells are shown in Fig. 1a and b. The device with a p-n junction on the rear surface consisted of an n-type crystalline silicon (c-Si) substrate, a p-type layer on the rear side to form a p-n junction, and a heavily doped n-type (n^+) layer on the front side to form a high-low junction. For another device with a p-n junction on the front surface, a p-type c-Si wafer was utilized as the substrate, covered by an n-type layer on the front side and a heavily doped p-type (p^+) layer on the rear side. A summary of the key input parameters used for the simulations is provided in Supporting Information (Table S1).

The EQE for various surface recombination velocities at the dual-side interfaces upon top and bottom illumination was calculated to demonstrate the significant impact of interface recombination on the optical response. The simulated results were divided into two parts based on the illumination direction and analyzed individually.

2.1. Upon top illumination (n-side)

In Fig. 2a, the EQE response across the entire wavelength range of 300 nm–1200 nm were enhanced by decreasing the surface recombination velocity at front interface (S_{front}) of n+/n junction from 200 cm/s to 0.7 cm/s in the rear-sided p-n junction silicon solar cell upon top illumination (n-side), resulting in an increase of short-circuit current density (J_{SC}) from 31.8 mA/cm^2 to 39.5 mA/cm^2, as shown in Fig. 2c. When S_{front} was set to 0.7 cm/s and the surface recombination velocity at the rear interface (S_{rear}) of the p-n junction decreased from 200 cm/s to 0.7 cm/s, the EQE response and J_{SC} did not exhibit any differences, as shown in Fig. 2b and **d**. These simulated results are highly consistent with the experimental findings outlined in the aforementioned studies [3–6], which are not difficult to explain. For any wavelength, there is stronger absorption at the incident side than at the opposite side, which roughly follows the Beer- Lambert law [13]. However, for long wavelengths, there was a much higher fraction of generation at the rear side than at short wavelengths. Upon top illumination (n-side), the incident light over the entire wavelength spectrum generates a large number of electron-hole pairs in the vicinity of the front interface, where the n+/n junction is located. However, only a small number of electron-hole pairs were generated in the vicinity of the rear interface, where the p-n junction was located, as shown in Fig. 3a. Owing to a weaker electric field at the high-low junction, a decrease in S_{front} enables more electron-hole pairs to be efficiently collected, ultimately contributing to the short-circuit current instead of recombination. Consequently, the EQE response over the entire wavelength range is enhanced as S_{front} decreases in the rear-sided p-n junction silicon solar cell upon top illumination. In contrast, because of the stronger electrical field at the p-n junction compared to the high-low junction, the electron-hole pairs are more effectively separated. Therefore, the alteration in S_{rear} had an insignificant influence on the optical response.

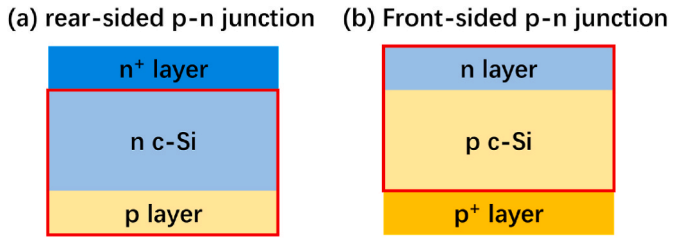

Fig. 1. Cross-sections of silicon solar cells with p–n junctions on a) rear and b) front surfaces.

2.2. Upon bottom illumination (p-side)

For the same solar cell, merely altering the illumination direction from top to bottom yielded significantly divergent outcomes. When S_{front} was decreased from 200 cm/s to 0.7 cm/s, an enhancement of the EQE response was observed solely in the long-wavelength range between 700 nm and 1200 nm with a slight increase in J_{SC} from 34.6 mA/cm^2 to 35.6 mA/cm^2, as depicted in Fig. 4a–c. This enhancement can be attributed to two facts: (i) long-wavelength light has a much higher fraction of generation at the rear side compared to short wavelengths, and (ii) a high-low junction does not separate electron-hole pairs as efficiently as a p-n junction, as illustrated in Fig. 3b. Therefore, the surface recombination velocity in the vicinity of the high-low junction primarily affects the optical response in the long-wavelength range. These findings are in close agreement with the published experimental results [6]. Notably, the optical response and photo-generated current remained unaffected by S_{rear} for the same reason discussed previously, as depicted in Fig. 4b and d. For the scenario involving a front-sided p-n junction silicon solar cell, identical simulations were performed, yielding similar results, which are provided in the Supporting Information (Figs. S1 and S2). It is to note that excellent surface passivation quality is standardly given in state-of-the-art high-efficiency heterojunction (HTJ) solar cells [14], so that the impact of different sensitivities of the surface recombination velocity on the EQE for front or rear junction solar cells is irrelevant for the efficiency that can be achieved today. This work is meant to provide guidelines for the quick diagnosis of "imperfect" passivation quality at the top and bottom interfaces of any type of solar cell. There are other reasons for using rear junctions instead of front junctions in high-efficiency HJT solar cells. A primary reason is that a thicker intrinsic silicon passivation and p-type contact layer is required on the p-side than the intrinsic silicon passivation and n-type contact layer on the n-side, so that the rear junction solar cell with the n-side on the front has lower parasitic absorption loss [15].

EQE measurements on the transparent passivating contact (TPC) and SHJ solar cells were performed to provide further strong evidence for the conclusions drawn from the simulation (Fig. S3). For the TPC cells with

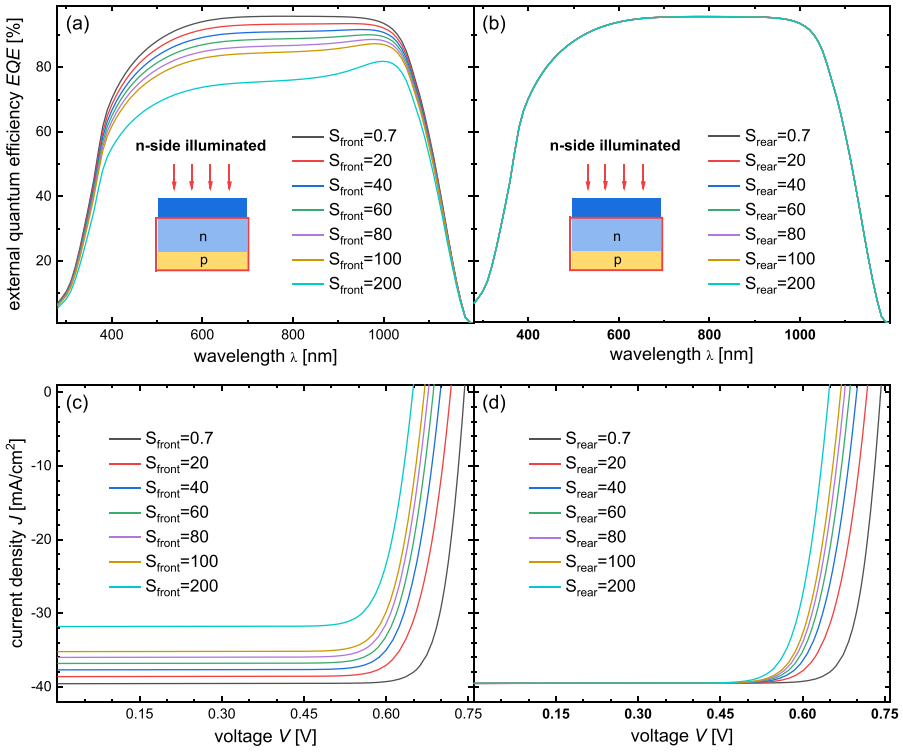

Fig. 2. Simulated EQE spectra of the rear-sided p-n junction silicon solar cell upon top illumination (n-side) as a function of surface recombination velocity at a) the front interface and b) the rear interface. Simulated *JV* curves of the rear-sided p-n junction silicon solar cell upon top illumination (n-side) as a function of surface recombination velocity at c) the front interface and d) the rear interface.

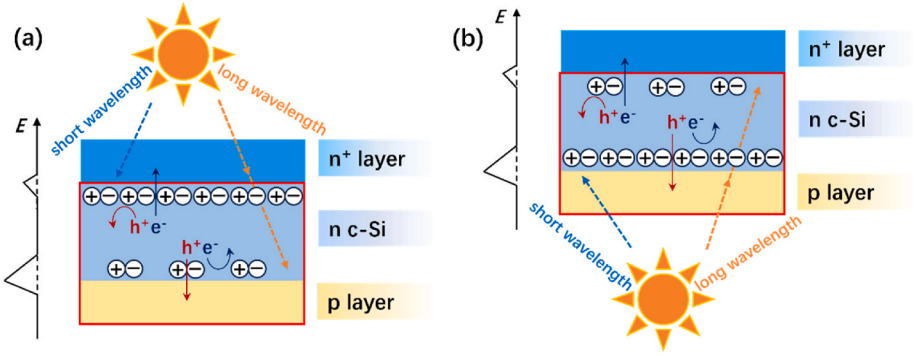

Fig. 3. Electron-hole pairs were generated in the rear-sided p-n junction silicon solar cell upon a) top illumination (n-side) and b) bottom illumination (p-side). Notably, the electric field of the p-n junction is stronger than that of the high-low junction, implying a more efficient separation of electron-hole pairs at the p-n junction.

front-sided high-low junctions, a decrease in the front surface recombination velocity ($S_{\text{eff\_front}}$) due to the thickness variation in the passivating nc-SiC:H layer enhanced the EQE response in the entire wavelength range upon top illumination. The $S_{\text{eff\_front}}$, implied open-circuit voltage (iV_{OC}), and efficiency (η) of TPC cells as a function of passivating nc-SiC:H layer thickness are provided in the Supporting Information (Table S2). For SHJ cells with a front-sided p-n junction, optical response enhancement was observed in the long-wavelength range with increasing thickness of the rear a-SiO_X:H <i> buffer layer because of the improvement in the passivation quality of the c-Si/a-SiOx:H rear interface.

2.3. Absorption at different wafer depth

The absorption profile in the modeled silicon solar cells as a function of wafer depth was also calculated by applying Beer–Lambert's law considering the wavelength-dependent absorption coefficient of silicon. This allows the investigation of the variation of absorption in different wavelength ranges at different locations of the silicon solar cells, which helps to better understand why the EQE enhancement is strongly related to the illumination direction and locations of interface recombination.

As shown in Fig. 5a, the absorption decreases with increasing wafer depth, with the majority occurring within a depth range of 40 μm. To analyze the contribution of different wavelength ranges to the absorption profile, Fig. 5b presents the absorption for incremental wavelength ranges as a function of the wafer depth. The wavelength range of 700 nm–1200 nm represents the infrared light spectrum (red curve). The wavelength range of 400 nm–1200 nm consists of infrared and visible light spectra (green curve). With the addition of the ultraviolet region, the range of 300 nm–1200 nm represents the entire spectrum (blue curve). Therefore, the colored areas between each curve represent the absorption for three wavelength ranges: infrared, visible, and

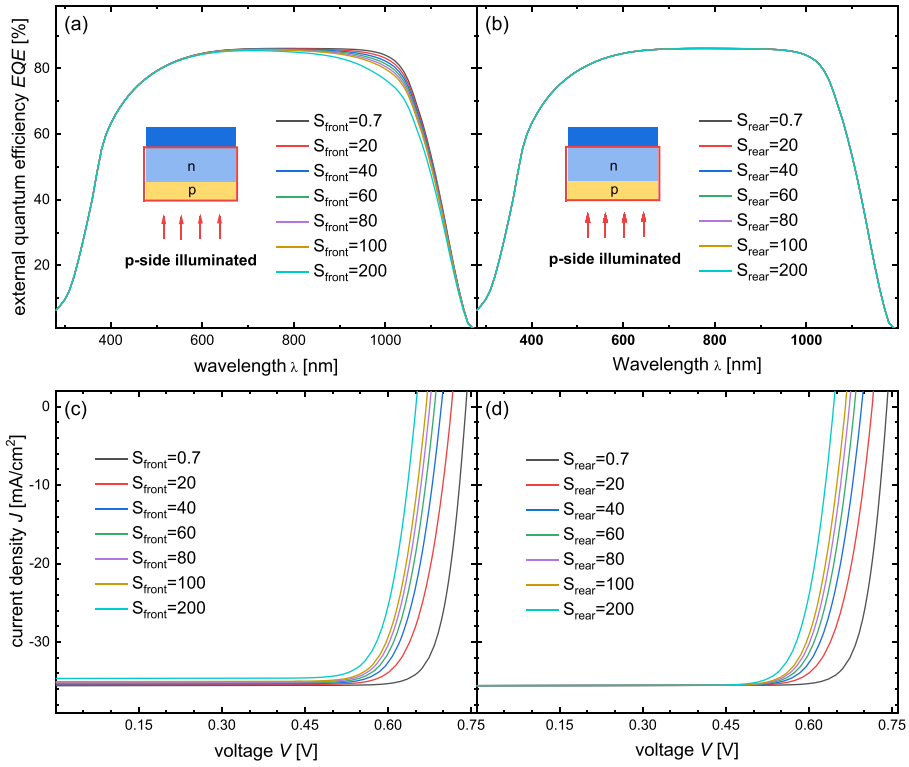

Fig. 4. Simulated EQE spectra of the rear-sided p-n junction silicon solar cell upon bottom illumination (p-side) as a function of surface recombination velocity at a) the front interface and b) the rear interface. Simulated *JV* curves of the rear-sided p-n junction silicon solar cell upon bottom illumination (p-side) as a surface function of recombination velocity at c) the front interface and d) the rear interface.

ultraviolet. A simple comparison of the integrated areas reveals that the visible light spectrum predominantly contributes to the total absorption with a maximum area of approximately 33000 r.u. μm, and the contribution from the ultraviolet spectrum (30 r.u. μm) is notably smaller than that of the other two spectra (Fig. S4). In addition, the absorptions of the three spectra at various depths in the modeled silicon solar cells are individually plotted in Fig. 5c to examine their respective threshold depths more closely.

In Fig. 5c, the absorption from the ultraviolet spectrum with the smallest contribution disappears a few micrometers from the sample surface, and its maximum absorption (A_{max}) is 22, as shown in Fig. 5b. The threshold depth, defined as the sample depth when the absorptance decreased to 1E-4 r.u., for the visible spectrum (400–700 nm) was approximately 40 μm with an A_{max} of 13371, suggesting that the majority of electron-hole pairs were generated from this spectral range and close to the illuminated surface. Conversely, incident light within the infrared spectrum (700 nm–1200 nm) is consistently absorbed along the silicon wafer, generating electron-hole pairs across nearly its entire thickness. Regardless of which side of the sample is illuminated, absorption from the infrared spectrum consistently contributes to the EQE and determines the optical response in the long-wavelength range. It is primarily the contributions from the visible spectrum that matter and change from top to bottom illumination. If the separation of electron-hole pairs generated by the visible spectrum is facilitated, allowing efficient collection of charge carriers, enhancement in the EQE response can be observed across the entire wavelength range. These results explain why EQEs exhibit much broader spectral response enhancement when the illumination direction is altered in some organic/inorganic solar cells. Moreover, leveraging the insights gleaned from these findings, the EQE response under dual-side illumination conditions can be used as a powerful tool for the quick diagnosis of the passivation quality at the top and bottom interfaces.

3. Conclusions

Numerical simulations were conducted to explore the impact of the surface recombination velocity at both the front and rear interfaces on the external quantum efficiency of silicon solar cells under top and bottom illumination. The simulated results of external quantum efficiency upon illumination from the high-low junction side demonstrate that regardless of the doping type of the silicon substrate, suppressing carrier recombination at the high-low junction interface enhances the optical response across the entire wavelength range. However, optical response enhancement only occurs in the long-wavelength range by decreasing the surface recombination velocity at the high-low junction interface according to the simulated external quantum efficiency upon illumination from the p-n junction side. The difference in the optical response enhancement can be attributed to two factors: (i) visible light is completely absorbed within a wafer depth of 40 μm, and only infrared light in the long wavelength range above 700 nm contributes to the rear-side absorption; and (ii) a high-low junction does not separate electron-hole pairs as efficiently as a p-n junction owing to a weaker electric field. These results are highly consistent with our experimental data for both SHJ and TPC solar cells, as well as the published experimental findings for various organic/inorganic solar cells [3–6]. From a practical point of view, if there is uncertainty about the passivation quality of either the front or rear interface, it is highly recommended to measure the external quantum efficiency from both sides of the device.

CRediT authorship contribution statement

Qing Yang: Writing – review & editing, Writing – original draft, Visualization, Validation, Resources, Project administration, Methodology, Investigation, Funding acquisition, Formal analysis, Data curation. **Karsten Bittkau:** Writing – review & editing, Visualization, Validation, Software, Resources, Project administration, Methodology,

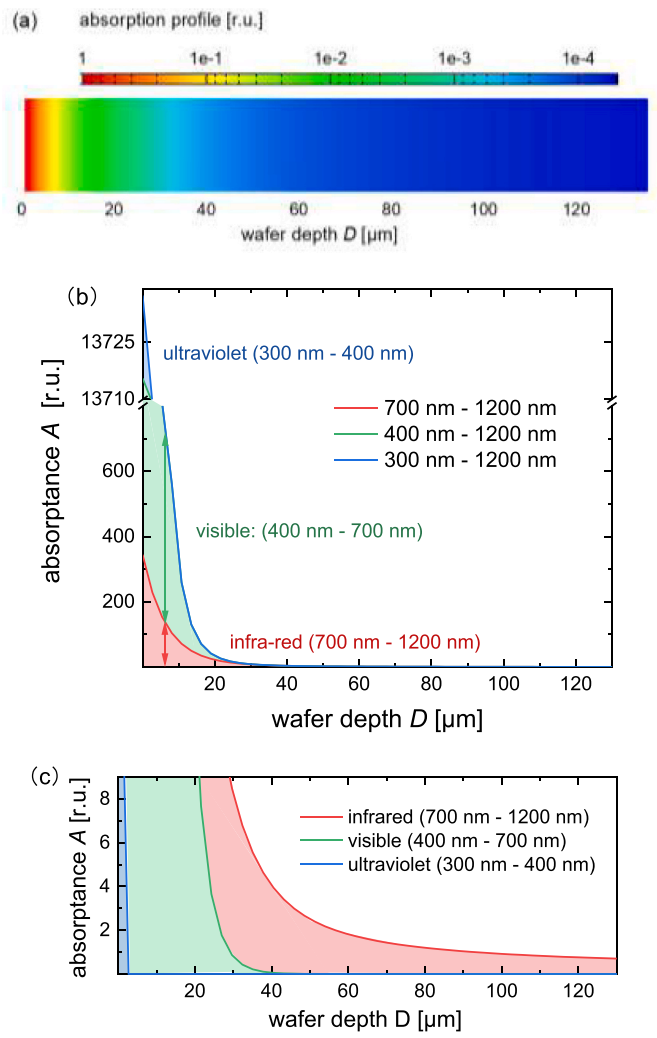

Fig. 5. a) Calculated absorption profile of modeled silicon solar cells as a function of wafer depth. b) Absorption for incremental wavelength ranges as a function of wafer depth. c) Absorption of three spectra (infrared, visible, and ultraviolet) as a function of wafer depth.

Investigation, Formal analysis, Data curation, Conceptualization. **Alexander Eberst:** Writing – review & editing, Resources, Investigation, Data curation. **Uwe Rau:** Supervision. **Kaining Ding:** Writing – review & editing, Supervision, Resources, Project administration, Investigation, Funding acquisition, Data curation, Conceptualization.

Declaration of competing interest

The authors declare that they have no known competing financial interests or personal relationships that could have appeared to influence the work reported in this paper.

Data availability

Data will be made available on request.

Acknowledgments

This work was supported by the German Federal Ministry of Economic Affairs and Energy in the framework of the TOP project under the grant number 03EE1080B. QY is grateful for the financial support from the China Scholarship Council (No. 202004910368).

Appendix A. Supplementary data

Supplementary data to this article can be found online at https://doi.org/10.1016/j.solmat.2024.112953.

References

[1] M. Wright, A. Uddin, Organic—inorganic hybrid solar cells: a comparative review, Sol. Energy Mater. Sol. Cells 107 (2012) 87–111.
[2] D. Abou-Ras, T. Kirchartz, U. Rau, Advanced Characterization Techniques for Thin Film Solar Cells, Wiley Online Library, 2011.
[3] P.M.P. Salomé, B. Vermang, R. Ribeiro-Andrade, J.P. Teixeira, J.M.V. Cunha, M. J. Mendes, S. Haque, J. Borme, H. Águas, E. Fortunato, R. Martins, J.C. González, J. P. Leitão, P.A. Fernandes, M. Edoff, S. Sadewasser, Passivation of interfaces in thin film solar cells: understanding the effects of a nanostructured rear point contact layer, Adv. Mater. Interfac. 5 (2017) 1701101.
[4] E. McVay, A. Zubair, Y. Lin, A. Nourbakhsh, T. Palacios, Impact of Al2O3 passivation on the photovoltaic performance of vertical WSe2 Schottky junction solar cells, ACS Appl. Mater. Interfaces 12 (2020) 57987–57995.
[5] M. Hatamvand, S. Gholipour, M. Chen, Y. Zhou, T. Jiang, Z. Hu, Y. Chen, W. Huang, Dual-side interfacial passivation of FAPbI3 perovskite film by Naphthylmethylammonium iodide for highly efficient and stable perovskite solar cells, Chem. Eng. J. 460 (2023) 141788.
[6] K. Ding, U. Aeberhard, F. Finger, U. Rau, Silicon heterojunction solar cell with amorphous silicon oxide buffer and microcrystalline silicon oxide contact layers, Phys. Status Solidi Rapid Res. Lett. 6 (2012) 193–195.
[7] A. Fell, A free and fast three-dimensional/two-dimensional solar cell simulator featuring conductive boundary and quasi-neutrality approximations, IEEE Trans. Electron. Dev. 60 (2013) 733–738.
[8] A. Fell, K.C. Fong, K.R. McIntosh, E. Franklin, A.W. Blakers, 3-D simulation of interdigitated-back-contact silicon solar cells with Quokka including perimeter losses, IEEE J. Photovoltaics 4 (2014) 1040–1045.
[9] A. Fell, K.R. McIntosh, M. Abbott, D. Walter, Quokka version 2: selective surface doping, luminescence modeling and data fitting, in: Proceedings of the 23rd International Photovoltaic Science and Engineering Conference, 2013.
[10] A. Richter, J. Benick, F. Feldmann, A. Fell, M. Hermle, S.W. Glunz, n-Type Si solar cells with passivating electron contact: identifying sources for efficiency limitations by wafer thickness and resistivity variation, Sol. Energy Mater. Sol. Cells 173 (2017) 96–105.
[11] A. Richter, J. Benick, A. Fell, M. Hermle, S.W. Glunz, Impact of bulk impurity contamination on the performance of high-efficiency n-type silicon solar cells, Prog. Photovoltaics Res. Appl. 26 (2018) 342–350.
[12] A. Richter, J. Benick, R. Müller, F. Feldmann, C. Reichel, M. Hermle, S.W. Glunz, Tunnel oxide passivating electron contacts as full-area rear emitter of high-efficiency p-type silicon solar cells, Prog. Photovoltaics Res. Appl. 26 (2017) 579–586.
[13] D.F. Swinehart, The beer-lambert law, J. Chem. Educ. 39 (1962) 333.
[14] W. Duan, A. Lambertz, K. Bittkau, D. Qiu, K. Qiu, U. Rau, K. Ding, A route towards high-efficiency silicon heterojunction solar cells, Prog. Photovoltaics Res. Appl. 30 (2021) 384–392.
[15] M. Köhler, M. Pomaska, P. Procel, R. Santbergen, A. Zamchiy, B. Macco, A. Lambertz, W. Duan, P. Cao, B. Klingebiel, S. Li, A. Eberst, M. Luysberg, K. Qiu, O. Isabella, F. Finger, T. Kirchartz, U. Rau, K. Ding, A silicon carbide-based highly transparent passivating contact for crystalline silicon solar cells approaching efficiencies of 24%, Nat. Energy 6 (2021) 529–537.